2022-03

High-quality reconstruction of China's natural streamflow

Miao, C

http://hdl.handle.net/10026.1/19252

10.1016/j.scib.2021.09.022
Science Bulletin
Elsevier BV

Supplementary materials for

High-quality reconstruction of China's natural streamflow

Contents of this Supplementary material

Supplementary Text 1

Water balance principle-based reconstruction method

Traditional naturalized-gauge streamflow reconstruction involves removal of major flow alterations caused by human activities from gauged discharges in order to approximate undisturbed natural conditions. Such alterations arise from river diversions, dams, sand dredging, irrigation schemes, flood protection works, land reclamation schemes, and other water management interventions. Natural streamflow is widely used as a database for understanding natural hydrological processes [1], assessing the impact of human activities on river flows [2], and calibration of hydrological models [3, 4]. The inferred natural streamflow records used to train the present hydrological model were provided by the Ministry of Water Resources of China. Herein, naturalized streamflow (Fig. 1) was reconstructed with additional water volume included from direct water abstraction, including agricultural irrigation, industrial consumption, domestic consumption, water diversion, and reservoir storage [2, 3], from:

$$W_n = W_m + W_{ir} + W_{iw} + W_{dw} \pm W_d \pm W_f \pm W_r \qquad (1)$$

where W_n is the naturalized streamflow volume; W_m is the measured streamflow volume at gauge stations; W_{ir} is the volume of water diverted from the river for irrigation; W_{iw} is the water volume extracted for industrial consumption; W_{dw} is the water volume removed for domestic consumption; W_d is the water volume diverted from the river to basins; W_f is the volume diverted for flood protection; and W_r is the consumption of water stored in reservoirs.

Supplementary Text 2

Detailed information for 330 stations

In this study, the 1961–1979 referred monthly natural streamflow data at 330 hydrological gauge stations of ten river basins across China (Fig. 1) were obtained from the Hydrological Yearbook of China and local water resources departments, and used to calibrate and validate the VIC hydrological model. As indicated in Fig. S2a, there are three types of streamflow record: (Type-1) naturalized records from the Bureau of Hydrology of the Ministry of Water Resources of China, obtained using the water balance principle (Supplementary Text 1); (Type-2) observed records from gauges without upstream dams; and (Type-3) observed records from gauges with upstream dams (see Fig. S2b for number of dams). Water management effects within Type-1 streamflow were fully removed by appropriate addition/subtraction of water abstraction volumes to/from the observed streamflow, including agricultural irrigation, industrial consumption, domestic consumption, water diversion, and reservoir storage (Supplementary Text 1). Nearly half of all gauge records (149 of 330 stations) belong to Type-1 (Fig. S2). The remaining gauge records are all near-natural with no upstream dams present (Type-2, 122 of 330 stations) or a low level of dam influence (Type-2, 59 of 330 stations Fig. S2). In summary, the referred calibration and validation data from these 330 gauge stations are of sufficient quality to reconstruct natural streamflow.

Supplementary Text 3

Parameter uncertainty analysis

The parameter uncertainty analysis framework involved: (1) parameter sensitivity analysis, (2) parameter optimization, and (3) parameter regionalization. Firstly, the parameter of importance was identified for each water resources region. Then the parameter of importance was optimized to minimize bias between modeled and inferred natural streamflow. Finally, the important parameter in ungauged areas was determined from the corresponding parameter at gauged catchments.

(1) Parameter sensitivity analysis (SA)

6000 training simulations were run for the period from 1960 to 1979 based on parameter combinations obtained by the Sobol′ sequence [5] sampling method for each of the 14 selected catchments from the 10 water resources regions. We applied four sensitivity analysis (SA) approaches – methods–sum-of-trees (SOT), multivariate adaptive regression splines (MARS), delta test (DT), and metamodel-based Sobol′ method (Sobol′) – to the 6000 parameter samples to calculate sensitivities, and thus identified the most important parameter out of 13 streamflow-related parameters. SOT, MARS, and DT are qualitative methods, which provide heuristic scores that intuitively represent the relative sensitivity of different parameters. Sobol′ is a quantitative SA method that indicates the sensitivity of a given parameter by computing its impact on the total variance of model output. The foregoing SA methods come from different algorithm designs. SOT derives from a random tree-based algorithm, which is fundamentally an additive model with multivariate components [6]. The importance of a parameter is determined by the total number of splits of that parameter in the SOT model. MARS makes use of linear regression, pairwise splines analysis, and binary recursive partitioning [7], with the primary influence of input parameters determined as the sum of all basis functions that involve only a single parameter. The DT method is based on the nearest neighbor principle for estimating the variance of the residuals [8], with parameter sensitivity represented by the distance between the parameter function value and the nearest point function value; the parameter subset with smallest DT criterion corresponds to the most important parameter subset. The metamodel-based Sobol′ method provides a precise estimate of the contribution ratio of each parameter to the total variance of model output [9]. By combining the foregoing four SA methods, accurate parameter screening is more likely to be achieved than by relying solely on any one method.

(2) Parameter optimization

After determining the important parameters, their values were tuned in the Variable Infiltration Capacity (VIC) model to match the inferred natural streamflow at 200 training stations during the calibration period (1961–1969). Then the model was run using the tuned parameters for the validation period (1970–1979), and the results compared against the inferred streamflow. Adaptive surrogate modeling-based optimization (ASMO) [10] carried out parameter calibration. ASMO facilitated searches for optimal parameters of complex models using a low number of true model runs. The ASMO algorithm comprised four steps: (i) initial sampling, (ii) surrogate model construction, (iii) surrogate model optimization, and (iv) adaptive sampling. At the sampling step, the Sobol′ sequence, a quasi-Monte Carlo sampling method, was used to obtain the initial sample sets. The initial sample size was set equal to 20 times the number of the sensitive parameters to be evaluated by SA. A Gaussian Processes method constructed the surrogate model according to the initial sample sets, and a global optimization algorithm, shuffled complex evolution [11], then optimized the constructed surrogate model to find the minimum of an error response surface in multi-parameter space. During adaptive sampling, the minimum interpolating surface method iteratively refined the surrogate model until convergence. Steps (iii) and (iv) were repeated until convergence criteria were met for parameter optimization of the actual physical model. We set the convergence criteria as either the objective function value of the VIC simulation remaining unchanged after a number of searches equal to 20 times the dimensionality of the parameters, or the number of searches reaching a prescribed maximum number of model runs, N_{max} (in this study $N_{max} = 500$, excluding initial samples). Please note that for each run of the actual physical model (up to a maximum of 500 runs), an additional ~1000 parameter optimizations were implemented using the constructed surrogate model by SCE-UA, resulting in a total maximum ~ 500×1000 trials for each catchment.

(3) Parameter regionalization

Parameter regionalization refers to parameter transfer strategies that estimate model parameter values for any ungauged catchment in a definable region of consistent hydrological response. The present study used multiscale Parameter Regionalization (MPR) (see [12]); this regionalization approach uses transfer functions to relate geophysical features at finest scale with model parameters at finest scale, and then upscale them to the selected modeling spatial scale (which is normally much coarser) [13]. Unlike conventional standard regionalization methods that define catchment predictors at modeling unit scale, MPR undertakes simultaneous regionalization for the sub-grid variability of catchment predictors [12]. By coupling the ASMO optimization algorithm with the MPR technique, we conducted simultaneous parameter estimation for both gauged and pseudo-ungauged catchments (Fig. S3). Details of the transfer function and upscale function of each model parameter are given in our previous work [14].

Supplementary Text 4

Skill metrics computation

Four skill metrics were used to evaluate model performance: Pearson's Correlation Coefficient (CC); Nash–Sutcliffe efficiency coefficient (NSE); Percent bias (Pbias, unit: %); and Kling-Gupta Efficiency coefficient (KGE). CC measures the linear correlation between modeled and observed streamflow, and is expressed:

$$\text{CC} = \frac{COV(Q_m, Q_o)}{\sigma Q_m \sigma Q_o} \tag{1}$$

where Q_m and Q_o are the modeled and observed streamflow respectively; COV is the covariance of Q_m and Q_o, and σQ_m and σQ_o are the standard deviations of the modeled and observed streamflow.

The NSE metric, which is widely used to determine overall model efficiency in hydrology [15], is computed from model-simulated and observed streamflow time series as follows:

$$\text{NSE} = 1 - \frac{\sum_{t=1}^{T}(Q_m^t - Q_o^t)^2}{\sum_{t=1}^{T}(Q_o^t - \overline{Q_o})^2} \tag{2}$$

where Q_m^t and Q_o^t are modeled and observed streamflows at time t. $\overline{Q_o}$ is the mean observed streamflow. NSE can range from $-\infty$ to 1, and the closer NSE is to 1, the more reliable is the match between modeled and inferred natural streamflow time series.

Pbias measures the percentage bias of modeled streamflow to be larger or smaller than the corresponding inferred natural streamflow, with 0 being perfect, and is given by:

$$\text{Pbias} = \sum \frac{Q_m - Q_o}{Q_o} \times 100 \tag{3}$$

KGE measures the Euclidean distance between a point and the optimal point that has CC, bias ratio (BR), and relative variability (RV) equal to 1 [16, 17], and is calculated from:

$$\text{KGE} = 1 - \sqrt{(CC-1)^2 + (BR+1)^2 + (RV-1)^2} \tag{4}$$

where

$$\text{BR} = \overline{Q_m}/\overline{Q_o} \tag{5}$$

and

$$\text{RV} = (\sigma Q_m/\overline{Q_m})/(\sigma Q_o/\overline{Q_o}) \tag{6}$$

KGE = 1 indicates perfect agreement between simulations and inferred natural streamflow.

Table S1. Characteristics of 13 streamflow-related parameters tested for sensitivity analysis and model optimization

Parameter	Brief description	Units	Range
B	Shape of the variable infiltration capacity curve controlling surface runoff	N/A	0.001–0.4 [a]
D_1	Thickness of upper soil layer	m	0.01–0.5 [b]
D_2	Thickness of middle soil layer	m	0.05–1.0 [a]
D_3	Thickness of bottom soil layer	m	0.5–2.5 [a]
Ds	Fraction of maximum velocity of baseflow	N/A	0.001–1 [a]
Dm	Maximum velocity of baseflow	mm/day	5–20 [a]
Ws	Fraction of maximum soil moisture content of bottom soil layer	N/A	0.1–1 [a]
E_1	Exponent of Brooks–Corey drainage equation for upper soil layer	N/A	8–30 [b]
E_2	Exponent of Brooks–Corey drainage equation for middle soil layer	N/A	8–30 [b]
E_3	Exponent of Brooks–Corey drainage equation for bottom soil layer	N/A	8–30 [b]
K_1	Saturated hydraulic conductivity in upper soil layer	mm/day	163–4765 [c]
K_2	Saturated hydraulic conductivity in middle soil layer	mm/day	163–4765 [c]
K_3	Saturated hydraulic conductivity in bottom soil layer	mm/day	163–4765 [c]

[a] Source: Shi and colleagues [18]

[b] Source: Demaria and colleagues [19]

[c] Source: Bennett and colleagues [20]

Table S2. Sensitive VIC model parameters for runoff simulations identified through sensitivity analysis.

Water resources region	**Sensitive parameters**
Songhua River	B, D_1, D_2, E_2
Liao River	B, D_1, D_2
Hai River	B, D_1, D_2, Ds, Ws, E_2
Yellow River	B, D_1, D_2, D_3, Ds, Ws
Huai River	D_1, D_2, E_2
Yangtze River	B, D_1, D_2, D_3, Ds, Ws
Southeast River drainage system	B, D_1, D_2, Ds, Ws
Pearl River	B, D_1, D_2, Ds, Ws
Southwest River drainage system	B, D_1, D_2, D_3, Ds, Ws, Dm
Northwest River drainage system	B, D_1, D_2, D_3, Ds, Ws, Dm

Table S3 Statistics of four performance metrics for training and test stations during the period from 1961 to 1979

Statistics	Training stations				Test stations			
	Performance metrics				Performance metrics			
	CC	Pbias (%)	NSE	KGE	CC	Pbias (%)	NSE	KGE
Maximum	0.99	65.75	0.98	0.97	0.99	84.49	0.93	0.92
Mean	0.93	13.9	0.81	0.75	0.89	26.55	0.68	0.59
Minimum	0.69	0.12	0.35	0.17	0.49	1.16	0.22	0.10

Note: Absolute values were used in calculating the statistics of the Pbias metric.

Table S4 Statistics of four performance metrics before and after model statistical post-processing during the period from 1961 to 1979 inclusive

Statistics	Before statistical post-processing				After statistical post-processing			
	Performance metrics				Performance metrics			
	CC	Pbias (%)	NSE	KGE	CC	Pbias (%)	NSE	KGE
Maximum	0.99	84.49	0.98	0.97	0.99	21.19	0.99	0.99
Mean	0.92	17.13	0.77	0.70	0.93	2.27	0.85	0.91
Minimum	0.49	0.12	0.22	0.10	0.45	0.01	0.09	0.40

Note: Absolute values were used in calculating the statistics of the Pbias metric.

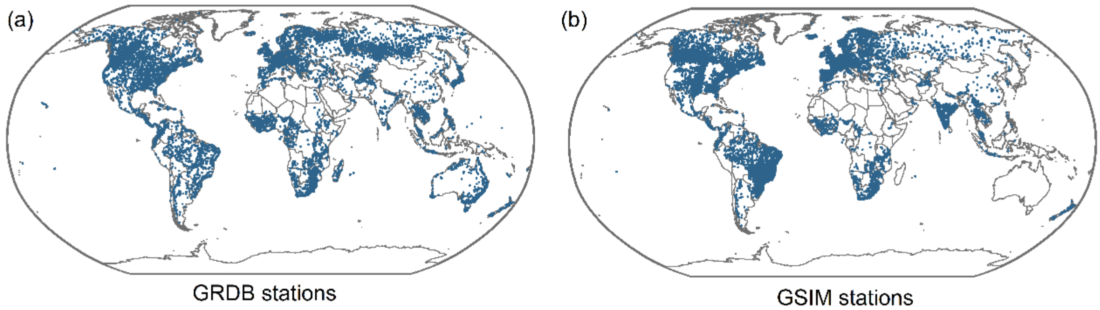

Fig. S1. Distribution of (a) Global Runoff Data Base (GRDB) hydrological stations and (b) Global Streamflow Indices and Metadata archive (GSIM) hydrological stations.

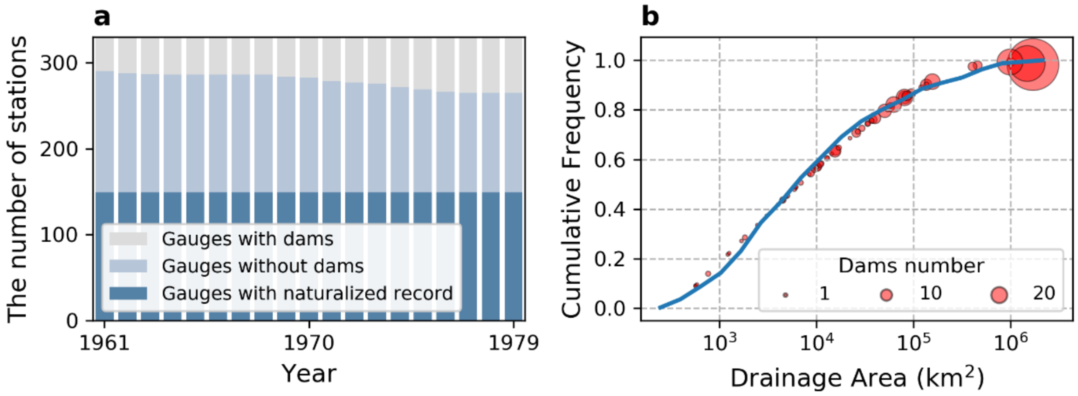

Fig. S2. Quality of data from 330 gauge stations. (a) Temporal changes in gauge numbers for three record groups: naturalized streamflow data obtained from the Ministry of Water Resources of China (dark blue bar), measured data without dam influence (light blue bar), or influenced by dams (grey bar). (b) Drainage area distribution for 330 gauge stations, with dam numbers of the third group (i.e., gauges influenced by dams) overlaid as red circles on the drainage area cumulative curve. The number of dams before 1979 was extracted from a dam-point dataset (GRanD v1.3, http://globaldamwatch.org/data/).

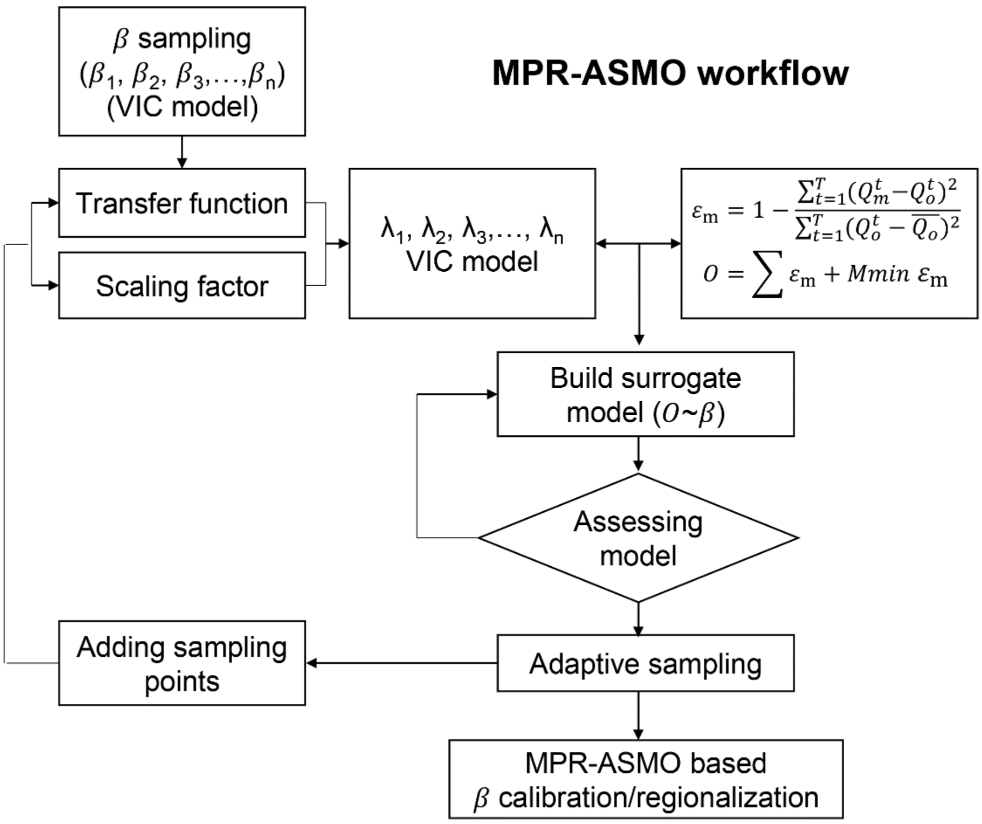

Fig. S3. Workflow diagram for combination of multiscale parameter regionalization (MPR) technique and ASMO algorithm.

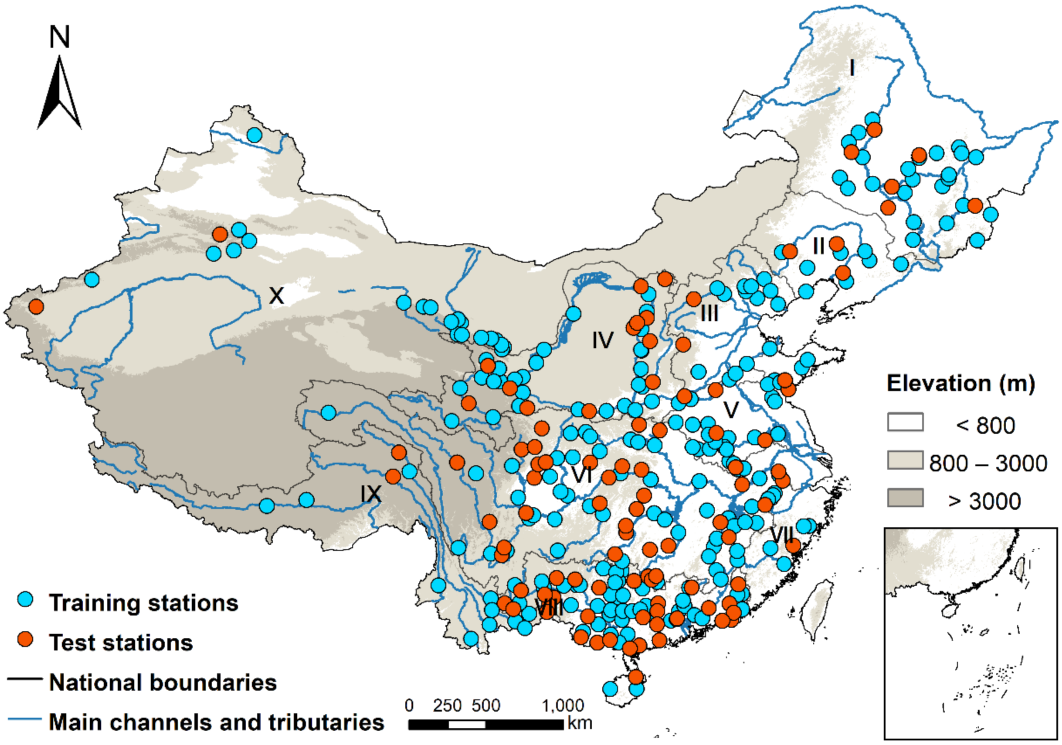

Fig. S4. Spatial distribution of training stations and test gauge stations.

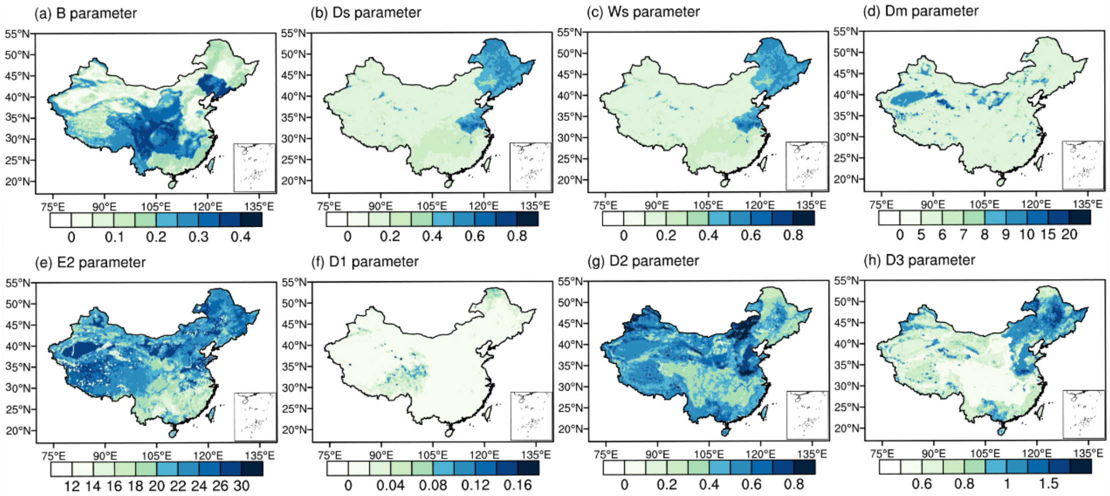

Fig. S5. Estimated seamless 0.25° × 0.25° model parameters obtained using the multiscale parameter regionalization technique: (a) B infiltration parameter; three baseflow parameters, (b) Ds, (c) Ws, and (d) Dm; the second-layer drainage parameter, (e) E2; and three soil thickness parameters, (f) D1, (g) D2, and (h) D3.

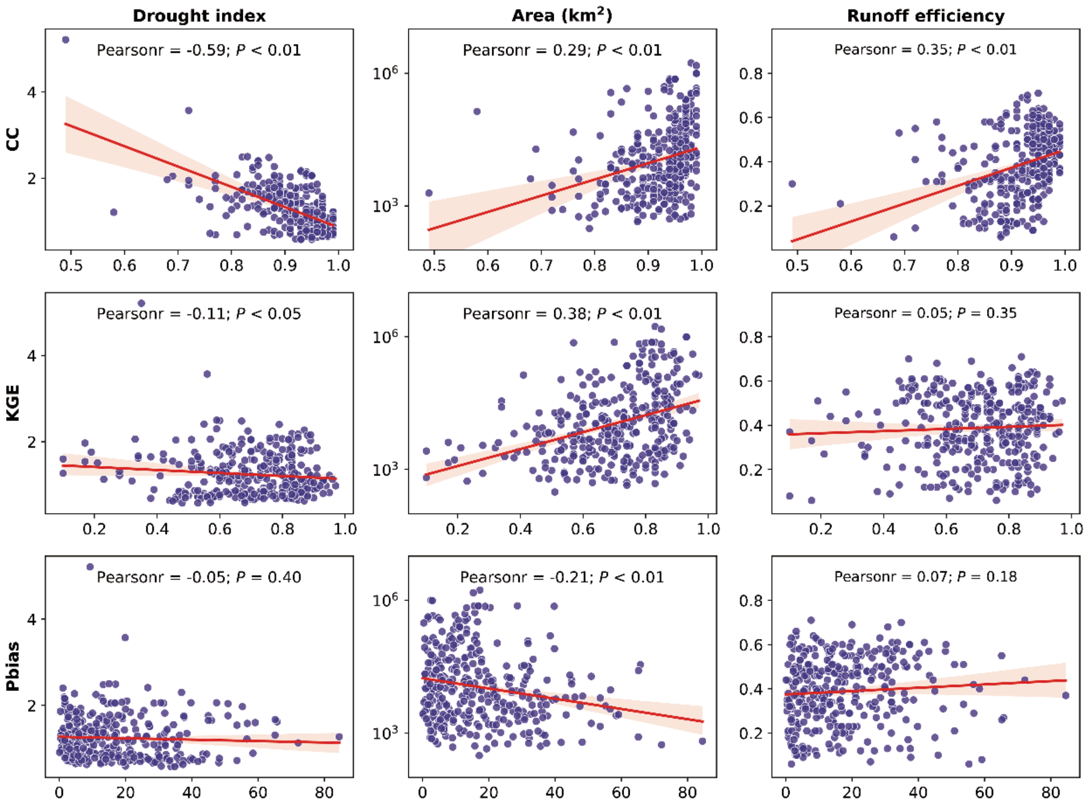

Fig. S6. Scatter plots and correlation relationships between CC, KGE, and Pbias metrics and drought index, area, and runoff efficiency for 330 gauge stations across China. Note that absolute values are used for the Pbias metric.

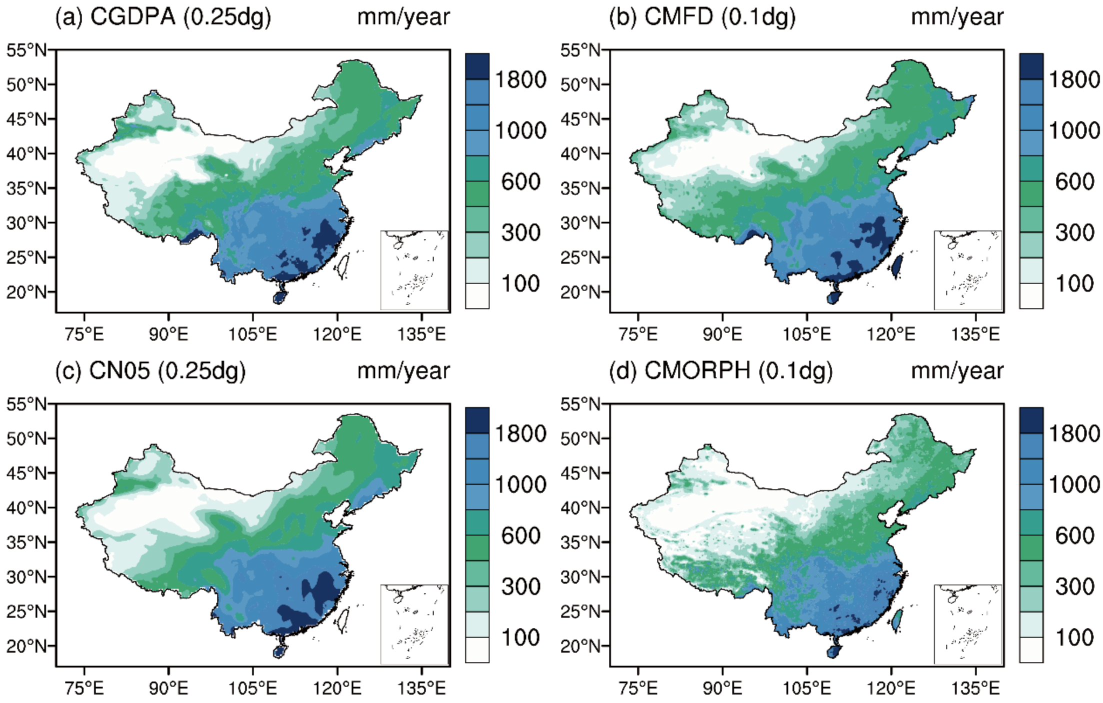

Fig. S7. Spatial distributions of multi-year mean annual precipitation obtained from (a) the China Gauge-based Daily Precipitation Analysis (CGDPA), (b) the China Meteorological Forcing Dataset (CMFD), (c) a high-quality gridded meteorological dataset based on ground observations (CN05.1), and (d) a high-resolution precipitation analysis based on gauge data and CMORPH satellite estimates (CMORPH) during the overlap period of 2008–2018. CGDPA datasets serve as model forcing in the present study.

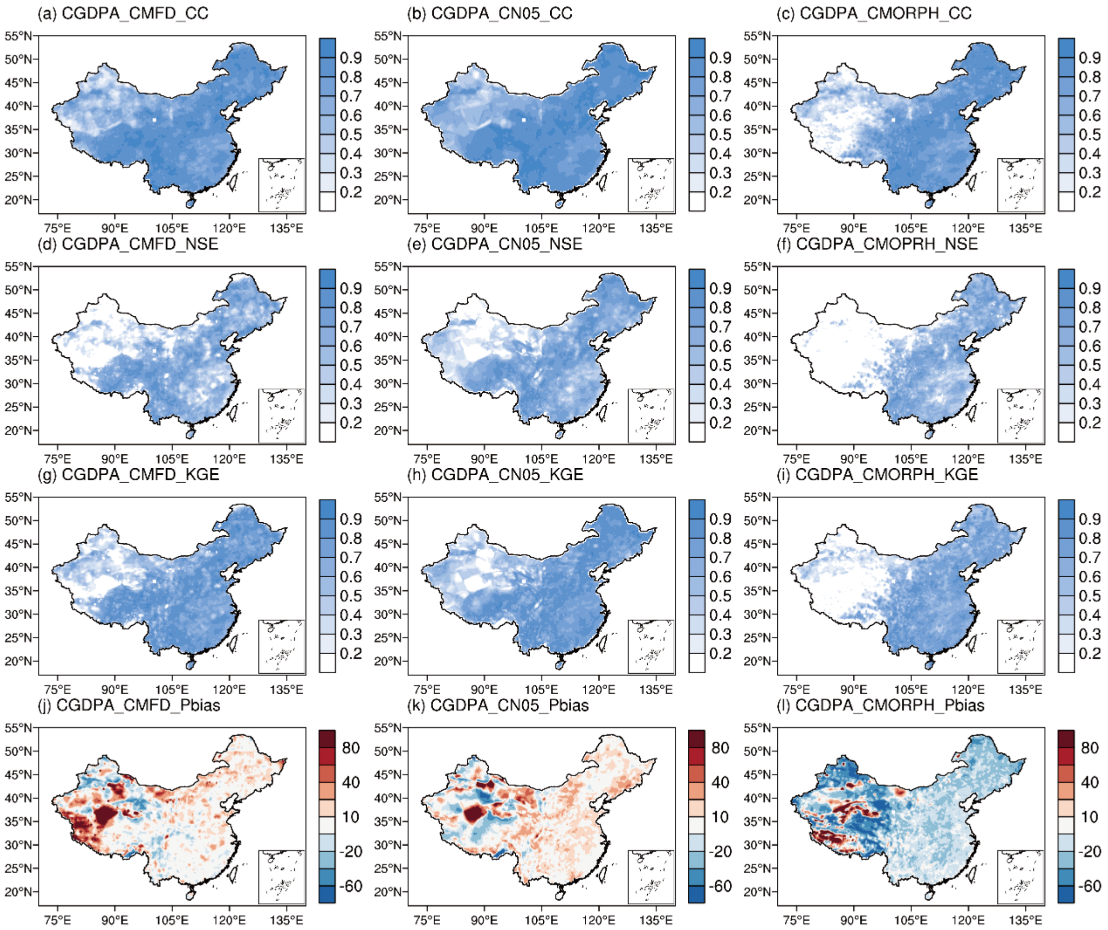

Fig. S8. Spatial distribution of CC, NSE, KGE, and Pbias between CGDPA and CMFD, CN05.1, and CMORPH precipitation products at monthly scale during the overlap period of 2008–2018. Subplot captions refer to precipitation product and the performance metric. For example, '(a) CGDPA_CMFD_CC' refers to the spatial correlation (CC) distribution for the CGDPA and CMFD monthly precipitation. CGDPA datasets served as forcing data in the present study.

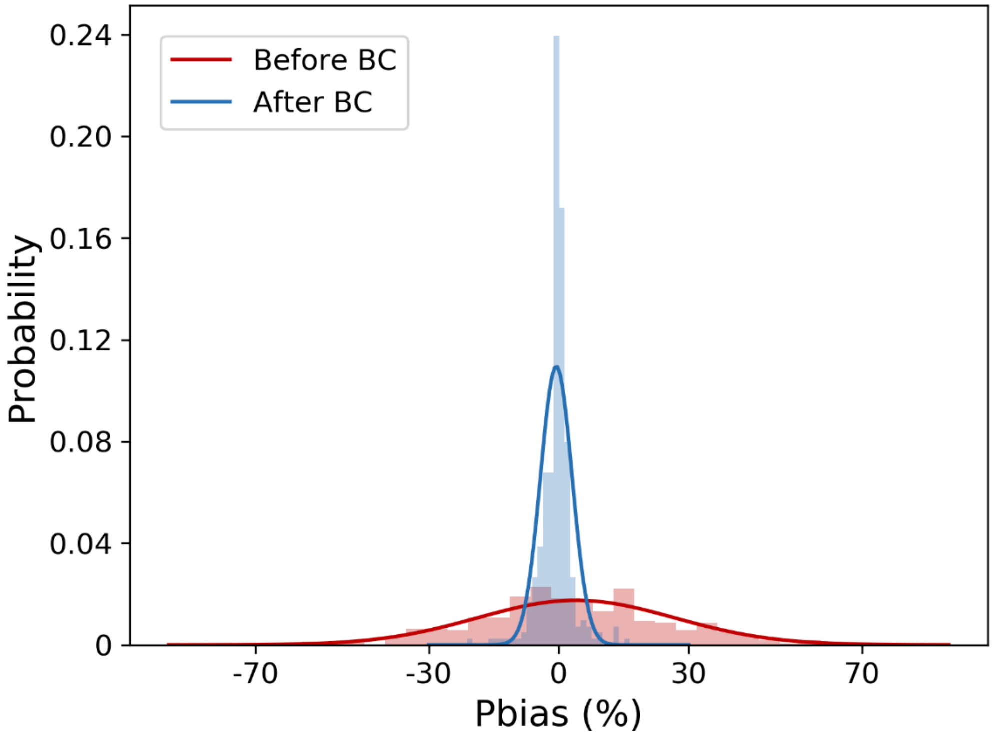

Fig. S9. Probability density function curves of Pbias metric before and after Bias Correction (BC) in the statistical post-processing procedure for data from 330 gauge stations across China.

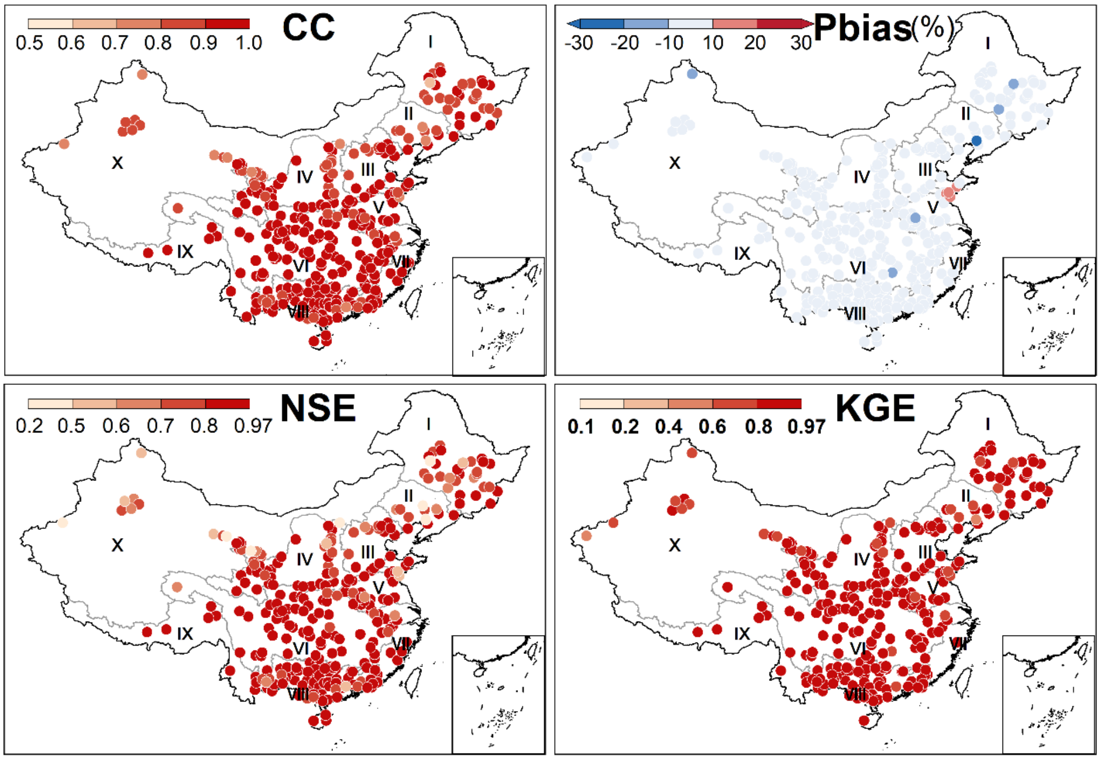

Fig. S10. Spatial pattern of four model performance metrics after model statistical post-processing during the period 1961 to 1979 inclusive. Gray boundaries indicate the 10 water resources regions of China: I, Songhua River; II, Liao River; III, Hai River; IV, Yellow River; V, Huai River; VI, Yangtze River; VII, Southeast River drainage system; VIII, Pearl River; IX, Southwest River drainage system; and X, Northwest River drainage system.

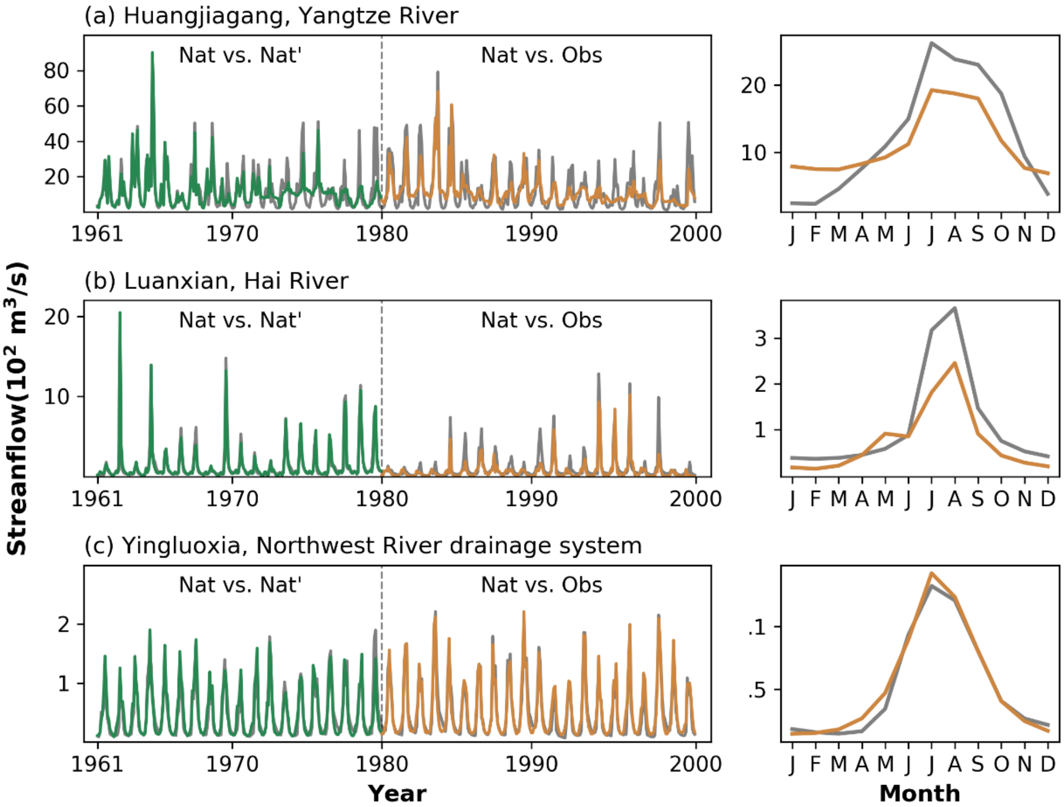

Fig. S11. Comparison of monthly streamflow time series and corresponding annual cycles between reconstructed natural streamflow and gauged streamflow at (a) Huangjiagang station, Yangtze River basin, (b) Luanxian station, Hai River basin, and (c) Yingluoxia station, Northwest River drainage system. Note that the annual cycles of monthly streamflow are plotted only for the period from 1980 to 2000. Nat, Nat' and Obs label the reconstructed natural streamflow, the referred natural streamflow, and the observed streamflow. The referred natural streamflow was calculated using the statistical water balance principle-based reconstruction method of the Ministry of Water Resources of China.

References

[1] Tu XJ, Singh VP, Chen XH, et al. Intra-annual distribution of streamflow and individual impacts of climate change and human activities in the Dongijang River Basin, China. Water Resour Manag, 2015; 29: 2677-95.

[2] Yuan X, Zhang M, Wang LY, et al. Understanding and seasonal forecasting of hydrological drought in the anthropocene. Hydrol Earth Syst Sci, 2017; 21: 5477-492.

[3] Gou JJ, Miao CY, Duan QY, et al. Sensitivity analysis-based automatic parameter calibration of the VIC model for streamflow simulations over China. Water Resour Res, 2020; 56: 1-19.

[4] Nijssen B, Lettenmaier DP, Liang X, et al. Streamflow simulation for continental-scale river basins. Water Resour Res, 1997; 33: 711-24.

[5] Sobol′ IM. On the distribution of points in a cube and the approximate evaluation of integrals. USSR Computational Mathematics and Mathematical Physics, 1967; 7: 86-112.

[6] Chipman HA, George EI, McCulloch RE. Bart: Bayesian additive regression trees. Ann Appl Stat, 2010; 4: 266-98.

[7] Friedman JH. Multivariate adaptive regression splines. Ann Stat, 1991; 19: 1-67.

[8] Pi H, Peterson C. Finding the embedding dimension and variable dependencies in time series. Neural Comput, 1994; 6: 509-20.

[9] Sobol' MI. Sensitivity estimates for nonlinear mathematical models. Matematicheskoe Modelirovanie, 1990; 1: 407–14.

[10] Wang C, Duan QY, Gong W, et al. An evaluation of adaptive surrogate modeling based optimization with two benchmark problems. Environ Model Softw, 2014; 60: 167-79.

[11] Duan QY, Sorooshian S, Gupta V. Effective and efficient gobal optimization for conceptual rainfall-runoff models. Water Resour Res, 1992; 28: 1015-31.

[12] Samaniego L, Kumar R, Attinger S. Multiscale parameter regionalization of a grid-based hydrologic model at the mesoscale. Water Resour Res, 2010; 46: 1-25.

[13] Mizukami N, Clark MP, Newman AJ, et al. Towards seamless large-domain parameter estimation for hydrologic models. Water Resour Res, 2017; 53: 8020-40.

[14] Gou JJ, Miao CY, Samaniego L, et al. CNRDv1.0: The China Natural Runoff Dataset version 1.0. Bull Amer Meteor Soc, 2021; 10.1175/BAMS-D-20-0094.1.

[15] Nash JE, Sutcliffe JV. River flow forecasting through conceptual models part I - a discussion of principles. J Hydrol, 1970; 10: 282-90.

[16] Lin PR, Pan M, Beck HE, et al. Global reconstruction of naturalized river flows at 2.94 million reaches. Water Resour Res, 2019; 55: 6499–516.

[17] Gupta HV, Kling H, Yilmaz KK, et al. Decomposition of the mean squared error and nse performance criteria: Implications for improving hydrological modelling. J Hydrol, 2009; 377: 80-91.

[18] Shi XG, Wood AW, Lettenmaier DP. How essential is hydrologic model calibration to seasonal streamflow forecasting? J Hydrometeorol, 2008; 9: 1350-63.

[19] Demaria EM, Nijssen B, Wagener T. Monte Carlo sensitivity analysis of land surface parameters using the Variable Infiltration Capacity model. J Geophys Res, 2007; 112: 1-15.
[20] Bennett KE, Blanco JRU, Atchley AL, et al. Global sensitivity of simulated water balance indicators under future climate change in the Colorado Basin. Water Resour Res, 2018; 54: 132-49.